

Study of nanoparticles based on Cr and Sb doped TiO₂ as pigments for inkjet technology applications

Marc Jovaní¹, María Domingo¹, Thales R. Machado^{1,2}, Elson Longo³, Héctor Beltrán Mir^{1,*}, Eloisa Cordoncillo¹.

¹Departamento de Química Inorgánica y Orgánica, Universitat Jaume I de Castellón, Avda. Sos Baynat s/n, 12071, Castellón de la Plana, Spain

²LIEC-Laboratório Interdisciplinar de Eletroquímica e Cerâmica, Departamento de Química, UFSCar-Universidade Federal de São Carlos, Rod. Washington Luis km 235, P.O. Box 676, 13565-905 São Carlos, São Paulo, Brazil

³LIEC-Laboratório Interdisciplinar de Eletroquímica e Cerâmica, Instituto de Química, UNESP-Universidade Estadual Paulista Júlio de Mesquita Filho, P.O. Box 355, 14801-907 Araraquara, São Paulo, Brazil

* Corresponding author: mir@uji.es, Tel. +37 964 728245, Fax +34 964 728214

Abstract

Nanoparticles of the ceramic pigment with composition Ti_{0.97}Cr_{0.015}Sb_{0.015}O₂ were prepared by microemulsion-mediated solvothermal method at 180 °C. Anatase or rutile single phase was obtained depending on the synthesis conditions. Scanning electron microscope analysis showed the formation of nanospheres with particle size around 600 nm. The anatase to rutile transformation temperature was determined by Raman spectroscopy. The evolution of the colour was studied, and it was related with the polymorphic transition. Yellow nanopigments were obtained at low temperature and huge orange colour was observed at high temperature. Nanopigments prepared at 180 °C were tested with an industrial frit. Similar chromatic coordinates of an industrial orange ceramic pigment obtained at high temperatures were observed. ζ-potential values of the nanoparticles were ~ -57 mV. The size, shape, colour and electrostatic stability of these nanoparticles make them potential candidates to be applied in glazes or inkjet printers as orange ceramic pigments.

Keywords: nanoparticles, pigment, titanium dioxide, orange ceramic pigment, inkjet

1-Introduction

Titanium dioxide, TiO_2 , has a wide range of applications. Since its commercial production in the early twentieth century, it has been widely used as a pigment [1], sunscreens [2,3], paints [4], toothpaste [5], etc. Titanium dioxide occurs mainly in three crystalline forms: rutile, anatase and brookite. Rutile is the stable phase, and anatase and brookite are metastable. Both anatase, space group $I4_1/amd$, and rutile, space group $P4_2/mnm$, are tetragonal. Structures consist of TiO_6 octahedra, sharing four edges in anatase and two edges in rutile [6,7].

Nowadays, the field of nanotechnology has generated a great deal of interest because materials have numerous new properties in nanosize-scaled. These size-dependent properties include new phase transition behaviour, different thermal and mechanical properties, interesting surface activity and reactivity, and unusual optical, electrical and magnetic characteristics [8–10]. In this way, and more closely in the field of nanopigments, TiO_2 have a massive potential market.

Ceramic nanopigments have been developed for inkjet decoration of ceramic tiles using quadrichromic technology, being a new field of application. The nanopigments are able to overcome some actual problems of the inkjet industrial processes [11]. The use of pigmenting particles at the nanoscale is necessary for inkjet applications [12,13]. At present in the industry, these nanoparticles are basically obtaining by different milling steps [14,15]. The use of nanopigments in inkjet technology can solved problems like nozzle clogging, dispersion or instability caused by micronized pigments, and moreover, remove the milling stages [16].

Wet chemistry methods are one of the best options to prepare TiO_2 nanoparticles. The literature reports approaches for the synthesis of nanoparticles of titania, including thermal hydrolysis [17,18], sol-gel [19,20], hydro/solvothermal method [21,22] and microemulsion processes [23,24]. Among them, solvothermal and microemulsion methods are extensively used for the preparation of nanomaterials.

Solvothermal method has many advantages such as:

- 1) The final product can be obtained directly at relatively lower reaction temperature.
- 2) Crystalline products with different composition, structure, and morphology could be prepared modifying the synthesis conditions like temperature, pH, times or reactant concentration.
- 3) It produces high purity particles compare with traditional solid-solid routes.
- 4) The equipment and processing required are simpler, and the control of the reaction conditions is easier than other methods.

Therefore, the solvothermal synthesis is a good method for the preparation of oxide ceramic fine powders [21]. However, large sizes of TiO₂ nanocrystals and poor dispersion stability are usually appear in the materials prepared by solvothermal methods.

Microemulsions with nanosized aqueous cores have been extensively used as the reaction media for preparation of nanomaterials [25,26]. TiO₂ nanomaterials prepared by micelle method have often amorphous structure, and calcination is usually necessary in order to induce high crystallinity [10].

Based on the advantages of each method, a combination of microemulsion with solvothermal method has been explored to prepare nanomaterials such as SrCO₃ nanostructures [27] or Ca₁₀(PO₄)₆(OH)₂ [28]. Shenm *et al.* [29] have successfully synthesized rutile and anatase with microemulsion-mediated hydrothermal method. They studied the preparation of rutile or anatase modifying the synthesis conditions such as the amount of urea in aqueous phase of the microemulsion. The effect of pH on TiO₂ phase structure have been also extensively studied [30,31]. Regarding these studies, the low pH favours the formation of rutile phase while more alkaline media favours anatase phase formation. Other studies were done in order to control the growth of the particles. In order to prevent grain growth of the nanoparticles, Somiya *et al.* [32] prepared nanomaterials by hydrothermal microemulsion process. They conclude that the aqueous micelles in microemulsions act as microreactors to confine the growth of TiO₂ powders.

1 As it mention before, TiO_2 has been widely used as a pigment. In the industry, where
2 the solid solution used is $\text{Ti}_{0.97}\text{Cr}_{0.015}\text{Sb}_{0.015}\text{O}_2$, the pigment is manufactured starting
3 from anatase with chromium (III) oxide as chromophore element and antimony (III)
4 oxide as counterions in presence of several mineralizers. In this case, the colour is
5 acquired by calcinations at high temperatures around 1200 °C, where the development
6 of the colour occurs during the anatase-rutile transformation [33]. Anatase to rutile
7 transformation is reconstructive, therefore, transformation involves breaking and
8 reforming bonds [7]. This reconstructive transformation involves a contraction of the c-
9 axis and involving a volume contraction around 8% [34].
10
11
12
13
14
15
16

17 In this work, nanoparticles of Cr,Sb-doped TiO_2 ceramic pigment were prepared by
18 microemulsion-mediated solvothermal method, being able to control the phase (anatase
19 or rutile) mediated the control of pH of the aqueous phase and the time of the
20 solvothermal treatment. Calcinations were unnecessary because the solvothermal
21 treatment promoting the crystallization under mild temperatures, obtaining the desired
22 phase at low temperature. Studies of the rutile-anatase transformation were also
23 conducted in this work. These Cr,Sb-doped TiO_2 nanoparticles obtained at low
24 temperatures would have potential applications in the field of ceramic inks.
25
26
27
28
29
30
31
32
33

34 **2-Experimental**

35
36
37
38 Samples of $\text{Ti}_{0.97}\text{Cr}_{0.015}\text{Sb}_{0.015}\text{O}_2$ solid solution were prepared by a microemulsion-
39 mediated solvothermal route. The synthesis procedure was as follows: first, 10 mL of
40 Triton X-100 (surfactant), 3 mL of n-hexanol (cosurfactant 98%) and 16 mL of
41 cyclohexane (Sigma-Aldrich, $\geq 99.5\%$) were mixed under magnetic stirring, making up
42 the oil phase. Second, 2 mL of TiCl_4 (Fluka, $\geq 99\%$) solution, previously prepared in an
43 acid medium of HCl 4M, 2 mL of H_2O and the specifics amounts of $\text{CrCl}_3 \cdot 6\text{H}_2\text{O}$
44 (Probus, 93%) and SbCl_3 (Sigma-Aldrich, $\geq 99\%$), together with the necessary amount
45 of urea (Fluka, $\geq 99.5\%$) to obtain the desired phase, were mixed under magnetic stirring
46 (aqueous phase). The amount of urea was fixed to 4.5g and 1.5g per gram of pigment to
47 obtain anatase (A) or rutile (R) single phase, respectively [29].
48
49
50
51
52
53
54
55
56
57

58 Then, the aqueous phase was added dropwise to the oil phase under stirring mediated a
59 peristaltic pump at room temperature, forming a clear microemulsion. The
60
61
62
63
64
65

1 microemulsion was mixed under magnetic stirring for 48 h and, then, placed in a
2 Teflon-lined stainless steel autoclave and heated at 180 °C in an oven for variable times.
3 The precipitate was collected by centrifugation and washed repeatedly with ethanol.
4 After this process, samples were dried in air at room temperature. A scheme of the
5 general preparation of the samples is shown in Fig. 1, and the different treatment
6 conditions used in each case (time and the amount of urea) are shown in Table 1.
7
8
9

10
11
12 It is well known that the anatase-rutile phase transition involves a volume contraction,
13 and it depends on variables such as size, morphology, etc. [7]. Therefore, in order to
14 study the anatase-rutile phase transition in these samples, the powder with anatase phase
15 obtained at 180 °C was annealed at different temperatures between 750 and 1080 °C for
16 2 hours and cooled slowly inside the furnace.
17
18
19
20
21

22
23 Powders of samples at 180 °C, where single phase and optimal colour were obtained,
24 were mixed with one industrial frit (4% in weight of the pigment) using water as a
25 dispersing medium. Then, the dispersion was applied to white twice-fire bodies, to
26 verify composition stability as a ceramic colorant. A commercial transparent frit was
27 chosen. The frit composition used is given in Table 2. After drying, the pieces were
28 fired in an electric kiln. The heat treatment applied, corresponds to a standard firing
29 cycle used in a ceramic tile industry where the highest temperature of the cycle was
30 1080 °C for 5 minutes. This cycle involve five steps: ramping to 800 °C in 18 min,
31 heating from 800 °C to glaze firing temperature in 17 min, 5 min hold at 1080 °C,
32 cooling to 600 °C in 20 min, and finally cooling to room temperature in 15 min.
33
34
35
36
37
38
39
40
41
42

43 *2.1 Characterization*

44
45
46
47 Phase analysis of the samples was performed by powder XRD using a Bruker D4
48 Endeavor diffractometer with CuK_α radiation. Data were collected by step-scanning
49 from $2\theta = 20$ to 70° with a step size of 0.05° and 1.5 s of counting time at each step.
50
51
52
53

54
55 Scanning electron micrographs of the samples were taken on a field emission scanning
56 electron microscope (SEM) JEOL 7001F, equipped with a spectrometer of energy
57 dispersion of X-ray (EDX) from Oxford instruments, using acceleration voltage = 15
58 kV. Samples for microstructures and microanalysis determinations were deposited in an
59
60
61
62
63
64
65

1 aluminium holder and sputtered by platinum. Dynamic Light Scattering (DLS,
2 ZetaSizer-NanoSeries Malvern Instruments, Malvern, UK) was also used to measure the
3 ζ -potential of the as-prepared powder samples.
4
5
6

7 Raman spectra were recorder on a RFS/100/S Bruker Fourier transform (FT-Raman)
8 spectrometer, with a Nd:YAG laser excitation light at 1064 nm in a spectral resolution
9 of 4 cm^{-1} , in order to confirm the polymorphic phase (anatase or rutile).
10
11
12

13 UV-Visible diffuse reflectance spectroscopy and colorimetric study of the glazed fired
14 samples were performed on a CARY 500 SCAN VARIAN spectrophotometer in the
15 200-800 nm range. BaSO_4 was used as a reference. Reflectance (R_∞) was converted to
16 absorbance (K/S) by the Kubelka-Munk equation: $K/S = 2(1 - R_\infty) \times 2 R_\infty^{-1}$ [35]. The
17 positions of the main absorbance peaks in the optical spectra were determined through a
18 deconvolution procedure that allowed obtaining more accurately values for the
19 electronic transitions. The CIELab colour parameters L^* , a^* , and b^* of the glazed fired
20 compositions and the anatase powders at different temperatures were determined by
21 coupling an analytical software for colour measurements to the Varian
22 spectrophotometer, using a standard illuminant D65, to differentiate the pigment in
23 terms of colour. L^* is the lightness axis [black (0) to white (100)], a^* is the green (<0)
24 to red (>0) axis, and b^* is the blue (<0) to yellow (>0) axis.
25
26
27
28
29
30
31
32
33
34
35
36
37
38

39 **3-Results and discussion**

40 *3.1- Optimization of the crystalline phase and microstructural characterization*

41
42
43
44
45
46
47
48
49
50
51
52
53
54
55
56
57
58
59
60
61
62
63
64
65
66
67
68
69
70
71
72
73
74
75
76
77
78
79
80
81
82
83
84
85
86
87
88
89
90
91
92
93
94
95
96
97
98
99
100
101
102
103
104
105
106
107
108
109
110
111
112
113
114
115
116
117
118
119
120
121
122
123
124
125
126
127
128
129
130
131
132
133
134
135
136
137
138
139
140
141
142
143
144
145
146
147
148
149
150
151
152
153
154
155
156
157
158
159
160
161
162
163
164
165
166
167
168
169
170
171
172
173
174
175
176
177
178
179
180
181
182
183
184
185
186
187
188
189
190
191
192
193
194
195
196
197
198
199
200
201
202
203
204
205
206
207
208
209
210
211
212
213
214
215
216
217
218
219
220
221
222
223
224
225
226
227
228
229
230
231
232
233
234
235
236
237
238
239
240
241
242
243
244
245
246
247
248
249
250
251
252
253
254
255
256
257
258
259
260
261
262
263
264
265
266
267
268
269
270
271
272
273
274
275
276
277
278
279
280
281
282
283
284
285
286
287
288
289
290
291
292
293
294
295
296
297
298
299
300
301
302
303
304
305
306
307
308
309
310
311
312
313
314
315
316
317
318
319
320
321
322
323
324
325
326
327
328
329
330
331
332
333
334
335
336
337
338
339
340
341
342
343
344
345
346
347
348
349
350
351
352
353
354
355
356
357
358
359
360
361
362
363
364
365
366
367
368
369
370
371
372
373
374
375
376
377
378
379
380
381
382
383
384
385
386
387
388
389
390
391
392
393
394
395
396
397
398
399
400
401
402
403
404
405
406
407
408
409
410
411
412
413
414
415
416
417
418
419
420
421
422
423
424
425
426
427
428
429
430
431
432
433
434
435
436
437
438
439
440
441
442
443
444
445
446
447
448
449
450
451
452
453
454
455
456
457
458
459
460
461
462
463
464
465
466
467
468
469
470
471
472
473
474
475
476
477
478
479
480
481
482
483
484
485
486
487
488
489
490
491
492
493
494
495
496
497
498
499
500
501
502
503
504
505
506
507
508
509
510
511
512
513
514
515
516
517
518
519
520
521
522
523
524
525
526
527
528
529
530
531
532
533
534
535
536
537
538
539
540
541
542
543
544
545
546
547
548
549
550
551
552
553
554
555
556
557
558
559
560
561
562
563
564
565
566
567
568
569
570
571
572
573
574
575
576
577
578
579
580
581
582
583
584
585
586
587
588
589
590
591
592
593
594
595
596
597
598
599
600
601
602
603
604
605
606
607
608
609
610
611
612
613
614
615
616
617
618
619
620
621
622
623
624
625
626
627
628
629
630
631
632
633
634
635
636
637
638
639
640
641
642
643
644
645
646
647
648
649
650
651
652
653
654
655
656
657
658
659
660
661
662
663
664
665
666
667
668
669
670
671
672
673
674
675
676
677
678
679
680
681
682
683
684
685
686
687
688
689
690
691
692
693
694
695
696
697
698
699
700
701
702
703
704
705
706
707
708
709
710
711
712
713
714
715
716
717
718
719
720
721
722
723
724
725
726
727
728
729
730
731
732
733
734
735
736
737
738
739
740
741
742
743
744
745
746
747
748
749
750
751
752
753
754
755
756
757
758
759
760
761
762
763
764
765
766
767
768
769
770
771
772
773
774
775
776
777
778
779
780
781
782
783
784
785
786
787
788
789
790
791
792
793
794
795
796
797
798
799
800
801
802
803
804
805
806
807
808
809
810
811
812
813
814
815
816
817
818
819
820
821
822
823
824
825
826
827
828
829
830
831
832
833
834
835
836
837
838
839
840
841
842
843
844
845
846
847
848
849
850
851
852
853
854
855
856
857
858
859
860
861
862
863
864
865
866
867
868
869
870
871
872
873
874
875
876
877
878
879
880
881
882
883
884
885
886
887
888
889
890
891
892
893
894
895
896
897
898
899
900
901
902
903
904
905
906
907
908
909
910
911
912
913
914
915
916
917
918
919
920
921
922
923
924
925
926
927
928
929
930
931
932
933
934
935
936
937
938
939
940
941
942
943
944
945
946
947
948
949
950
951
952
953
954
955
956
957
958
959
960
961
962
963
964
965
966
967
968
969
970
971
972
973
974
975
976
977
978
979
980
981
982
983
984
985
986
987
988
989
990
991
992
993
994
995
996
997
998
999
1000

1 are shown in Fig 2 (a) and (b), respectively. The crystalline phase evolution of TiO₂ was
2 observed in both cases. Single phase of rutile [JCPDS 21-1276] was obtained when the
3 treatment time was higher than 17 hours and the amount of urea was fixed to 1.5 g, Fig
4 2(a). Secondary phase of anatase [JCPDS 21-1272] was identified at short times of
5 reaction. Therefore, the reaction needs more than 17 h for the formation of rutile single
6 phase. When the amount of urea was adjusted to 4.5 g, anatase single phase was
7 observed by XRD at short solvothermal treatment times, Fig 2(b). Secondary phase of
8 rutile appeared when the reaction time was increasing. R3 and R2 samples shown single
9 phase of rutile, and A1 sample shown single phase of anatase. R2 and A1 samples were
10 chosen to continue the study due to both samples presents single phase by XRD and the
11 shortest reaction times.
12
13
14
15
16
17
18
19
20
21

22 In order to confirm the results obtained by XRD, TiO₂ powders were further
23 characterized by Raman spectroscopy. Fig 3 shows the Raman spectra of R2 and A1,
24 showing the characteristic bands of the rutile and anatase single phase, respectively
25 [36]. Peaks located at 235, 432 and 602cm⁻¹ can be assigned to the rutile phase, Fig
26 3(a). No peaks that could be assigned to anatase TiO₂ or brookite were detected. In
27 contrast, peaks located at 157, 392, 507 and 628 cm⁻¹, Fig 3(b), can be assigned to the
28 anatase phase, and no other peaks were observed. Peaks that could be assigned to the
29 doping oxides, such as Cr₂O₃, located at 550 cm⁻¹ [37], were not found. These results
30 were consistent with the XRD results shown in Fig 2.
31
32
33
34
35
36
37
38
39

40 Products prepared by ceramic method at high temperature must be milled to adjust the
41 grain size of the pigments in function of their applications. It is important to know the
42 microstructure and grain size of the samples to select one or other application. For
43 example, grain sizes of below the micra are required for inkjet applications [11].
44 Therefore, the average grain size of the R2 and A1 samples were analyzed by SEM.
45 Micrographs and the grain size distribution of both powder samples are shown in Fig 4.
46 In both cases, there was no evidence of secondary phases by EDX, and therefore,
47 single-phase of Cr,Sb-TiO₂ solid solutions were obtained. Spherical nanoparticles were
48 observed and the grain size distribution was around 600 nm in both samples. The
49 production of inkjet inks involves a problem of the pigment sedimentation in the
50 dispersant [11]. In this way, measurements of ζ-potential were performed in water with
51 0.1% of sodium hexametaphosphate (65-70%, Aldrich) [38], in order to determine the
52
53
54
55
56
57
58
59
60
61
62
63
64
65

1 electrostatic stabilization of the R2 and A1 samples. Values of the ζ -potential were -57
2 mV and -56.5 mV, respectively. These negative values showed that the pigment can be
3 dispersed, avoiding the sedimentation. ζ -potential values around 20 mV are obtained for
4 the industrial pigment using glycol as dispersant [16]. Note that high ζ -potential values
5 (positive or negative) are better to avoid sedimentation and therefore, to be applied in
6 inkjet technology.
7
8
9
10

11 12 *3.2. Study of the anatase-rutile transformation and evaluation of the colouring* 13 *performance of the pigment* 14 15 16

17
18 The anatase-rutile phase transition involves a volume contraction, and it depends on
19 variables such as size, morphology, etc. [7]. In this work, Sb,Cr-doped TiO₂
20 nanospheres with anatase phase (A1), obtained at 180 °C, were fired at different
21 temperatures between 750 and 1080 °C to study the anatase-rutile phase transition. The
22 evolution of the colour with the phase transition was also studied. Raman spectra were
23 analyzed at each temperature and the chromatic coordinates were obtained. Fig. 5 shows
24 the evolution with temperature of the TiO₂ polymorphs by Raman spectroscopy. The
25 anatase-rutile transformation occurred at temperatures higher than 850 °C, and it was
26 essentially completed at 1000 °C. The chromatic coordinates of the samples at different
27 temperatures are shown in Table 3 and Fig 6. A1 sample presents a slight yellow
28 coloration at 180 °C. It is possible to relate the increase of a^* and b^* chromatic
29 coordinates with the phase transitions between 750 °C and 1080 °C. The b^* coordinate
30 increase from 23 to 36 suggesting that there is a relation between the polymorph
31 transformation and the increase of b^* coordinate. However, the a^* coordinate show an
32 approximately linear increase with temperature over the range 750 – 1000 °C. It is
33 important to highlight a constant b^* value in the interval between 900 and 1000 °C. In
34 this range, the main polymorph is rutile but anatase phase exist as minor phase. These
35 results suggest that the phase transformation is still going on at this range of
36 temperatures, probably due to the necessary time for the reconstruction of the structure,
37 from anatase to rutile. After the reconstructive transformation was occurred, and single
38 phase of rutile was obtained at 1080°C, the value of b^* increase significantly.
39
40
41
42
43
44
45
46
47
48
49
50
51
52
53
54
55
56
57
58
59
60
61
62
63
64
65

1
2
3
4
5
6
7
8
9
10
11
12
13
14
15
16
17
18
19
20
21
22
23
24
25
26
27
28
29
30
31
32
33
34
35
36
37
38
39
40
41
42
43
44
45
46
47
48
49
50
51
52
53
54
55
56
57
58
59
60
61
62
63
64
65

In order to assess the morphology of the powders during the phase transformation, SEM analysis was made at each temperature. Fig 7 shows the micrographs for the evolution of the morphology at different temperatures. Shape of the particles was different depending on the polymorph. When anatase is presented, the particles were almost spherical with certain agglomeration, Fig 7(a) and (b). During the transition, when rutile phase was the majority phase, the particles were rectangular. This fact suggests the elongation of the particles in the polymorphic transition.

3.3. Stability of the nanoparticles as a pigment

In order to determine the stability of the nanopowders prepared at 180 °C after glazing, a nanopowder/frit mixture was prepared and fired according the cycle set out in the experimental part at the maximum temperature of 1080 °C. The pieces with the glaze were also characterized by UV-Vis and values of the CIELab parameters were obtained. Diffuse reflectance spectra of A1, R2 and a commercial ceramic pigment fired at higher temperatures (>1200 °C) and glazed in the same conditions are presented in Fig 8 for the 230-800 nm wavelength range. Three main absorption bands are identified in the three spectra after the deconvolution: a broad band located at high energy and centred at ~260 nm attributed at the metal-ligand charge transfer ($Ti^{4+} \leftrightarrow O^{2-}$); a second band centred at ~340 nm corresponding to the substitution of the Ti(IV) by Cr(III) in an octahedral coordination ($Ti^{4+} \leftrightarrow Cr^{3+}$); and finally, a band centred at ~410 nm attributed to the *d-d* transition of the Cr(III) [${}^4A_2({}^4F) \rightarrow {}^4T_1({}^4F)$] in an octahedral coordination [39]. The intensity of this low energy band was different depending of the sample. Higher absorption of the *d-d* transition ${}^4A_2({}^4F) \rightarrow {}^4T_1({}^4F)$ was observed for the anatase (A1) glazed sample and this intensity was similar to the glazed commercial pigment. The precursor of titanium in solid-solid reactions is usually anatase, which transforms to rutile during the synthesis at high temperatures [40]. The intensity of the absorption bands could be related with the chromatic coordinates shown in Table 4. Good chemical and thermal stability into the frit was obtained and pigments acquired orange colour after glazing with the frit for both samples. Chromatic coordinates were slightly higher for the A1 and similar to those obtained for the commercial ceramic pigment in glaze (similar a^* values). Photographs of the samples before and after mixed with the frit are

1 shown in Fig 9. In summary, the colour of both samples in a standard frit was similar to
2 the coloration of the commercial ceramic pigment obtained at high temperatures.
3

4
5 This novel method of synthesise nanospheres at low temperature presents a lot of
6 benefits in front the method used in the ceramic industry. In the ceramic industry is
7 necessary the use of high temperatures calcinations to prepare rutile-based orange
8 pigments by the solid state method, requiring consumption of large amounts of energy.
9 Secondary phases are normally obtained from this method, not allowing a control of the
10 phases, the shape and size. A milling stage must be implemented to adjust the grain size
11 of the pigment due to the high particle size caused by high-temperature calcinations. For
12 this reasons, the novel synthesis method presented in this work to prepare nanopigments
13 at low temperature allows several advantages compared to the traditional solid-solid
14 method, used in the ceramic industry. A possible application of this method in the
15 industry can produce great economic benefits, removing the milling stage and saving a
16 high amount of energy in the calcinations at high temperature.
17
18
19
20
21
22
23
24
25
26
27

28 **4. Conclusions**

29
30
31
32
33 Anatase and rutile single phase of a yellow ceramic pigment based on Cr,Sb-TiO₂
34 were obtained by microemulsion mediated solvothermal method at 180 °C. The
35 experimental conditions were optimised in order to obtain anatase or rutile phase. These
36 samples prepared at 180 °C were single phase by XRD, Raman spectroscopy and
37 SEM/EDX. The solvothermal treatment time needed to obtain single phase of anatase or
38 rutile in the Ti_{0.97}Cr_{0.015}Sb_{0.015}O₂ solid solution was 17 h and 24 h, respectively.
39 Nanospheres were formed in both cases with an average particle size of 600 nm and a ζ-
40 potential value around -57 mV. The polymorphic transition temperature and the changes
41 of the morphology that this transformation involves were determined by Raman and
42 SEM. The anatase-rutile transformation occurred at temperatures higher than 850 °C,
43 and it was essentially completed at 1000 °C. Elongation of the particles in the
44 polymorphic transition was observed. There is also a correlation between the polymorph
45 transformation and the increase of the chromatic coordinates measured by UV-Vis,
46 leading to a huge orange colour pigment. Samples have a good chemical and thermal
47 stabilization into the frit, presenting similar chromatic coordinates to those of the
48 commercial ceramic pigment obtained at high temperatures, especially when the anatase
49
50
51
52
53
54
55
56
57
58
59
60
61
62
63
64
65

1
2
3
4
5
6
7
8
9
10
11
12
13
14
15
16
17
18
19
20
21
22
23
24
25
26
27
28
29
30
31
32
33
34
35
36
37
38
39
40
41
42
43
44
45
46
47
48
49
50
51
52
53
54
55
56
57
58
59
60
61
62
63
64
65

solid solution at 180 °C was the starting nanopowder. Orange colour was kept after the application on glazes. Therefore, the size, shape, colour and the electrostatic stability of these nanoparticles make it a potential candidate for orange ceramic pigment to be incorporated in the inkjet technology.

5. Acknowledgements

We thank the “Universitat Jaume I”-project No. P1 1B2013-65 (MJ, MD, HB, EC) for financial support. M.J. also thanks this project for a fellowship. We also thank to Juan Carlos Gallard (Ferro Spain S.A.) for the initial ideas.

6. References

- [1] Pfaff G, Reynders P. Angle-Dependent Optical Effects Deriving from Submicron Structures of Films and Pigments. *Chem Rev* 1999;99:1963–1981.
- [2] Salvador a, Pascual-Martí MC, Adell JR, Requeni a, March JG. Analytical methodologies for atomic spectrometric determination of metallic oxides in UV sunscreen creams. *J Pharm Biomed Anal* 2000;22:301–306.
- [3] Zallen R, Moret MP. The optical absorption edge of brookite TiO₂. *Solid State Commun* 2006;137:154–157.
- [4] Juergen H. Braun, Andrejs Baidins REM. TiO₂ pigment technology: a review. *Prog Org Coatings* 1992;20:105–138.
- [5] Yuan S, Chen W, Hu S. Fabrication of TiO₂ nanoparticles/surfactant polymer complex film on glassy carbon electrode and its application to sensing trace dopamine. *Mater Sci Eng C* 2005;25:479–485.
- [6] Mo S-D and Ching Y. Electronic and optical properties of three phases of titanium dioxide: Rutile, anatase, and brookite. *Phys Rev* 1995;51:23–32.
- [7] Hanaor D a. H, Sorrell CC. Review of the anatase to rutile phase transformation. *J Mater Sci* 2010;46:855–874.
- [8] Braginsky L, Shklover V. Light absorption in TiO₂ nanoparticles. *Eur Phys JD* 1999;630:627–630.
- [9] Beydoun D, Amal R. Implications of heat treatment on the properties of a magnetic iron oxide-titanium dioxide photocatalyst. *Mater Sci Eng B* 2002;94:71–81.
- [10] Chen X, Mao SS. Titanium dioxide nanomaterials: synthesis, properties, modifications, and applications. *Chem Rev* 2007;107:2891–2959.

- 1
2
3
4
5
6
7
8
9
10
11
12
13
14
15
16
17
18
19
20
21
22
23
24
25
26
27
28
29
30
31
32
33
34
35
36
37
38
39
40
41
42
43
44
45
46
47
48
49
50
51
52
53
54
55
56
57
58
59
60
61
62
63
64
65
- [11] Dondi M, Bloisi M, Gardini D, Zanelli C. Ceramic pigments for digital decorations inks:an overview. Castellon:Qualicer; 2012
 - [12] Monrós G. El Color de la cerámica: nuevos mecanismos en pigmentos para los nuevos procesados de la industria cerámica. Castelló de La Plana: Publicacions de la Universitat Jaume I. Servei de Comunicació i Publicacions; 2003.
 - [13] Feldmann C, Jungk H-O. Polyol-Mediated Preparation of Nanoscale Oxide Particles. *Angew Chemie Int Ed* 2001;40:359–362.
 - [14] Baldi G, Bitossi M, Barzanti A. US Patent 2008,7316741 B2
 - [15] Cavalcante PMT, Dondi M, Guarini G, Raimondo M, Baldi G. Colour performance of ceramic nano-pigments. *Dye Pigment* 2009;80:226–232.
 - [16] Davide Gardini, Michelle Dondi, Anna Luisa Costa, Francesco Matteucci, Magda Bloisi, Carmen Galassi, Giovanni Baldi and EC. Nano-Sized Ceramics Inks for Drop-on-Demand Ink-Jet Printing in Quadrichromy. *J Nanosci Nanotechnol*. 2008;8:1979–1988.
 - [17] Zhong Z, Ang T, Luo J, Gan H, Gedanken A, Materials A V, et al. Synthesis of One-Dimensional and Porous TiO₂ Nanostructures by Controlled Hydrolysis of Titanium Alkoxide via Coupling with an Esterification Reaction.*Chem Mater* 2005;17:6814–6818.
 - [18] Song KC, Pratsinis SE. Control of Phase and Pore Structure of Titania Powders Using HCl and NH₄OH Catalysts. *J Am Ceram Soc* 2001;84:92–98.
 - [19] Tayade RJ, Kulkarni RG, Jasra R V. Photocatalytic Degradation of Aqueous Nitrobenzene by Nanocrystalline TiO₂. *Ind Eng Chem Res* 2006;45:922–927.
 - [20] Murakami Y, Matsumoto T, Takasu Y. Salt Catalysts Containing Basic Anions and Acidic Cations for the Sol - Gel Process of Titanium Alkoxide: Controlling the Kinetics and Dimensionality of the Resultant Titanium Oxide. *J Phys Rev B* 1999;103:1836–1840.
 - [21] Cheng H, Ma J, Zhao Z, Qi L. Hydrothermal Preparation of Uniform Nanosize Rutile and Anatase Particles. *Chem Mater* 1995;7:663–671.
 - [22] Li G, Gray KA, August R V, Re V, Recei M, No V. Preparation of Mixed-Phase Titanium Dioxide Nanocomposites via Solvothermal Processing. *Chem Mater* 2007;19:1143–1146.
 - [23] Lal M, Chhabra V. Preparation and characterization of ultrafine TiO₂ particles in reverse micelles by hydrolysis of titanium di-ethylhexyl sulfosuccinate. *J Mater Res* 1998;13:1249–1254.
 - [24] Andersson M, Lars O. Preparation of Nanosize Anatase and Rutile TiO₂ by Hydrothermal Treatment of Microemulsions and Their Activity for Photocatalytic Wet Oxidation of Phenol. *J Phys Chem B* 2002;106:10674–10679.

- 1
2
3
4
5
6
7
8
9
10
11
12
13
14
15
16
17
18
19
20
21
22
23
24
25
26
27
28
29
30
31
32
33
34
35
36
37
38
39
40
41
42
43
44
45
46
47
48
49
50
51
52
53
54
55
56
57
58
59
60
61
62
63
64
65
- [25] Wu M, Long J, Huang A, Luo Y. Microemulsion-Mediated Hydrothermal Synthesis and Characterization of Nanosize Rutile and Anatase Particles. *Langmuir* 1999;15:8822–8825.
 - [26] Lu C-H, Wu W-H, Kale RB. Microemulsion-mediated hydrothermal synthesis of photocatalytic TiO₂ powders. *J Hazard Mater* 2008;154:649–654.
 - [27] Cao M, Wu X, He X, Hu C. Microemulsion-Mediated Solvothermal Synthesis of SrCO₃ Nanostructures. *Langmuir* 2005;21:6093–6096.
 - [28] Cao M, Wang Y, Guo C, Qi Y, Hu C. Preparation of ultrahigh-aspect-ratio hydroxyapatite nanofibers in reverse micelles under hydrothermal conditions. *Langmuir* 2004;20:4784–4786.
 - [29] Shen X, Zhang J, Tian B. Microemulsion-mediated solvothermal synthesis and photocatalytic properties of crystalline titania with controllable phases of anatase and rutile. *J Hazard Mater* 2011;192:651–657.
 - [30] Aruna ST, Tirosh S, Zaban a. Nanosize rutile titania particle synthesis via a hydrothermal method without mineralizers. *J Mater Chem* 2000;10:2388–2391.
 - [31] Yin S, Hasegawa H, Maeda D, Ishitsuka M, Sato T. Synthesis of visible-light-active nanosize rutile titania photocatalyst by low temperature dissolution–reprecipitation process. *J Photochem Photobiol A Chem* 2004;163:1–8.
 - [32] Sōmiya S, Roy R. Hydrothermal synthesis of fine oxide powders. *Bull Mater Sci* 2000;23:453–460.
 - [33] Matteucci F, Cruciani G, Dondi M, Raimondo M. The role of counterions (Mo, Nb, Sb, W) in Cr-, Mn-, Ni- and V-doped rutile ceramic pigments. *Ceram Int* 2006;32:385–392.
 - [34] Batzill M, Morales EH, Diebold U. Influence of Nitrogen Doping on the Defect Formation and Surface Properties of TiO₂ Rutile and Anatase. *Phys Rev Lett* 2006;96:1–4.
 - [35] S.Marfunin, *Physics of Minerals and Inorganic Materials*, Springer, Berlin, Heidelberg, New York, 1979.
 - [36] Chang H, Huang PJ. Thermo-Raman Studies on Anatase and Rutile. *J Raman Spectrosc* 1998;29:97–102.
 - [37] Sammelselg V, Tarre a., Lu J, Aarik J, Niilisk a., Uustare T, et al. Structural characterization of TiO₂–Cr₂O₃ nanolaminates grown by atomic layer deposition. *Surf Coatings Technol* 2010;204:2015–2018.
 - [38] Wakeman RJ, Marchant JQ. The influence of pH and temperature on the rheology and stability of aqueous titanium dioxide dispersions *Chem Eng J* 1997;67:97–102.

1 [39] Ishida, Shingo, Masahiko Hayashi YF and KF. Spectroscopic Study of the
2 Chemical State and Coloration of Chromium in Rutile. J Am Ceram Soc
3 1990;73:3351–3355.

4 [40] Gargori C, Cerro S, Galindo R, Monrós G. In situ synthesis of orange rutile
5 ceramic pigments by non-conventional methods. Ceram Int 2010;36:23–31.
6
7
8
9
10
11
12
13
14
15
16
17
18
19
20
21
22
23
24
25
26
27
28
29
30
31
32
33
34
35
36
37
38
39
40
41
42
43
44
45
46
47
48
49
50
51
52
53
54
55
56
57
58
59
60
61
62
63
64
65

Figure captions

1
2
3 **Fig. 1.** Scheme of the TiO₂ sample preparation.

4
5 **Fig. 2.** XRD patterns of TiO₂ synthesised with different amounts of urea and different times of
6 reaction at 180°C in order to prepare rutile (a) or anatase (b) phases.

7
8 **Fig. 3.** Raman spectra for TiO₂ samples prepared with (a) 1.5g of urea and after 24 h of
9 reaction, R2, and (b) 4.5g of urea and after 17h of reaction, A1. Rutile or anatase phases
10 were observed in (a) and (b), respectively.

11
12 **Fig. 4.** SEM images of A1 (a) and R2 (b) powder samples with the average particle size in each
13 case.

14
15 **Fig. 5.** Raman spectra of A1 sample fired at different temperatures.

16
17 **Fig. 6.** CIELab chromatic coordinates of the A1 powder fired at different temperatures.

18
19 **Fig. 7.** Micrographs of the A1 sample at different temperatures: (a) 750, (b) 800, (c) 850 and (d)
20 900°C.

21
22 **Fig. 8.** Diffuse Reflectance spectra for R2 (a), A1 (b) and a commercial ceramic pigment (c)
23 after glazing with deconvolution of optical bands.

24
25 **Fig. 9.** Photographs of the ceramic tiles for R2 (a), A1 (b) and the commercial pigment (c) after
26 mixed with the frit.

Highlights

- Nanoparticles of Cr,Sb-doped TiO₂ ceramic pigment were prepared by a microemulsion-mediated solvothermal method at 180 °C.
- Anatase and rutile single phase were synthesized modifying the pH of the aqueous phase and the time of the solvothermal treatment.
- Nanospheres with particle size around 600 nm were obtained.
- Nanopigments prepared at low temperature were tested with an industrial frit presented huge orange colour.
- The size, shape, colour and the electrostatic stability of these nanoparticles make it a potential candidate to be used in inkjet applications like a pigment.

Graphical abstract

Nanospheres based on Cr,Sb-doped TiO_2 with a potential use in the inkjet technology were obtained at low temperature (180 °C).

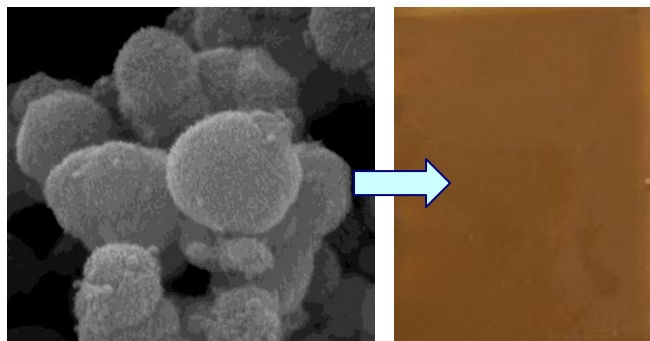


Figure 1

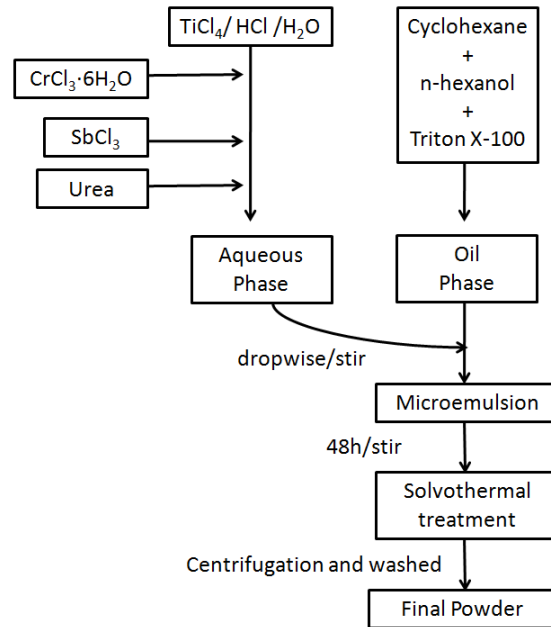


Fig 1.

Figure 2

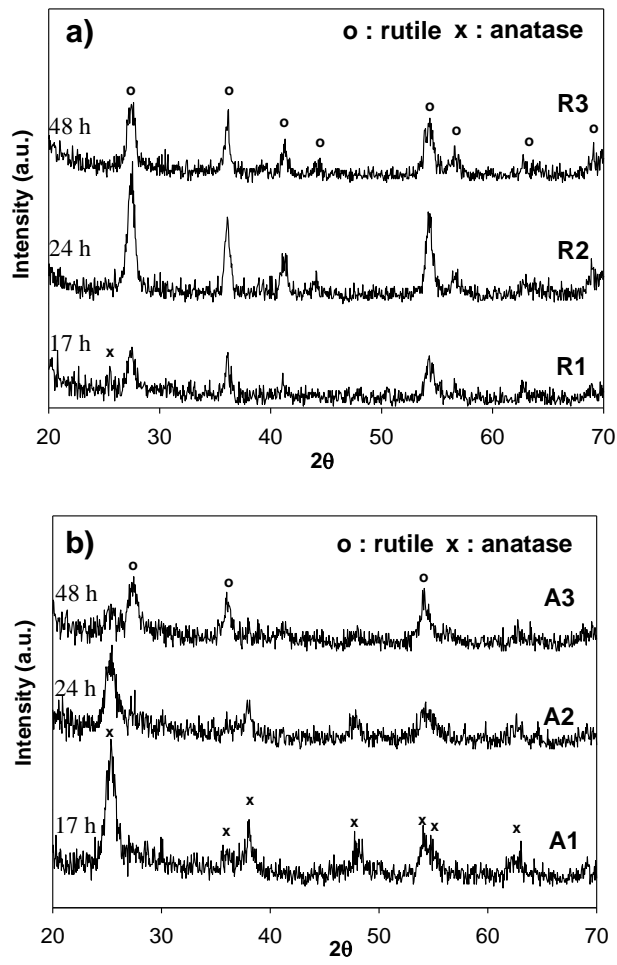


Fig 2.

Figure 3

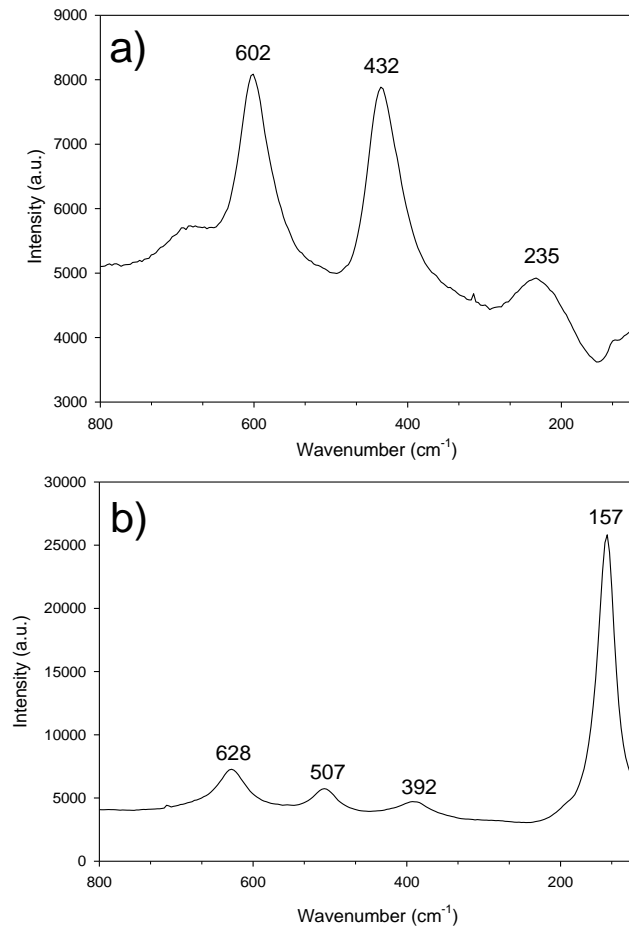


Fig 3.

Figure 4

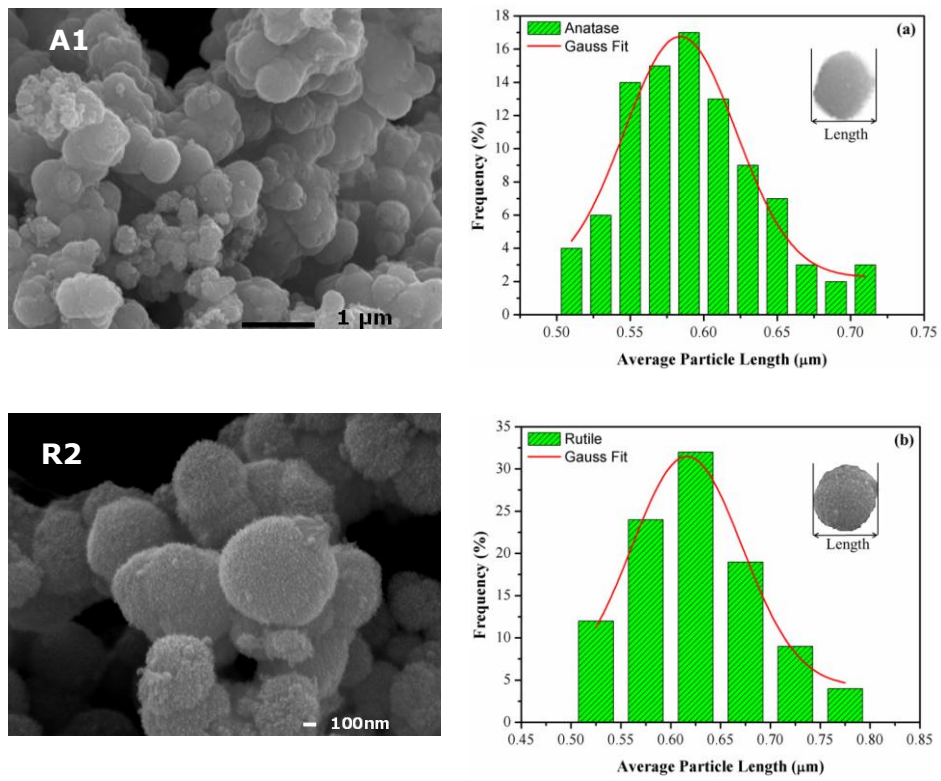


Fig 4.

Figure 5

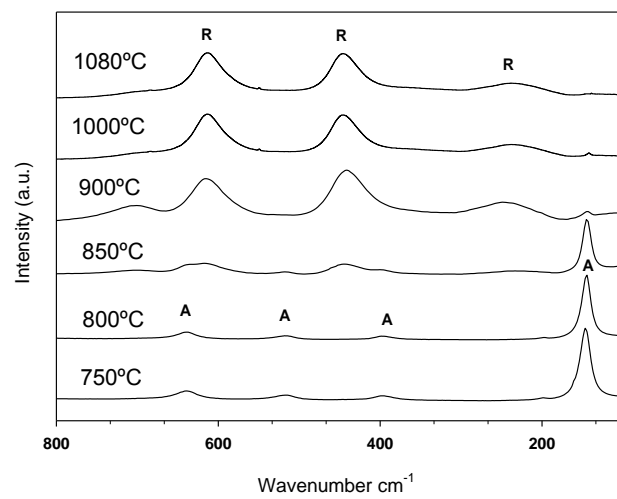


Fig 5.

Figure 6

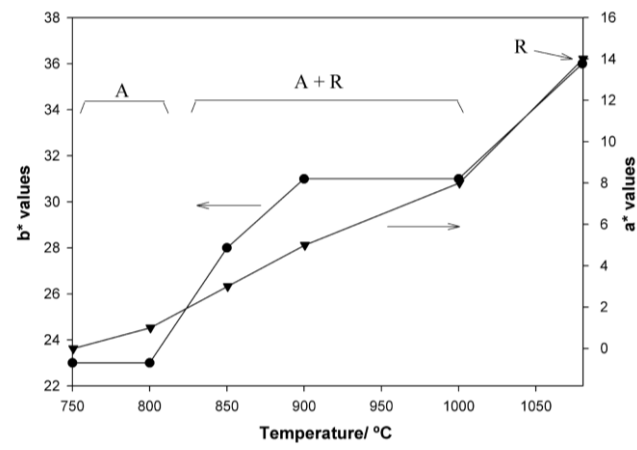


Fig 6.

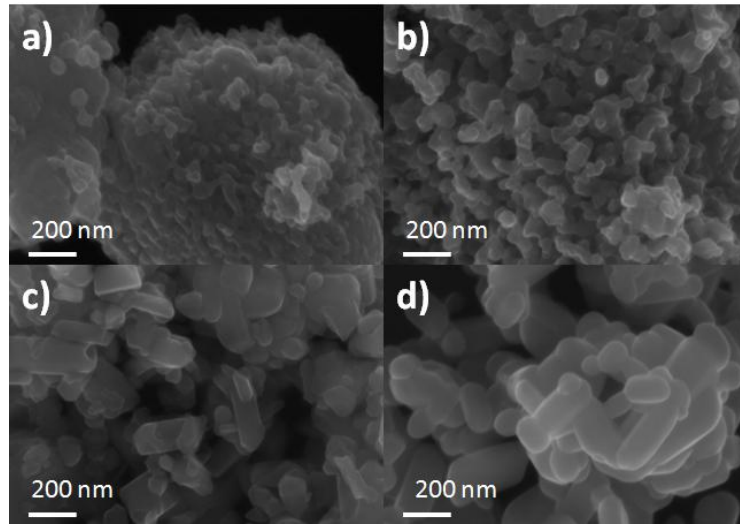


Fig 7.

Figure 8

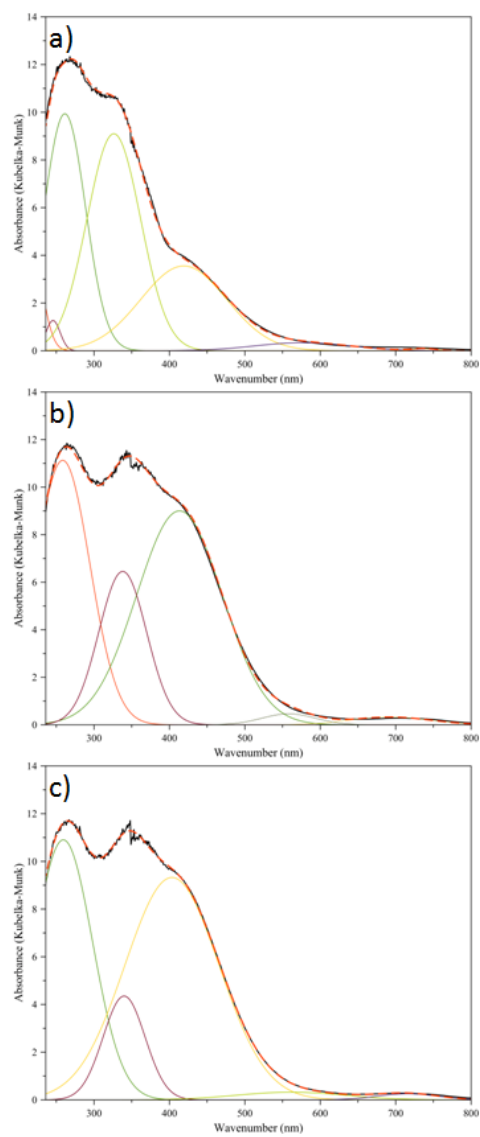


Fig 8.

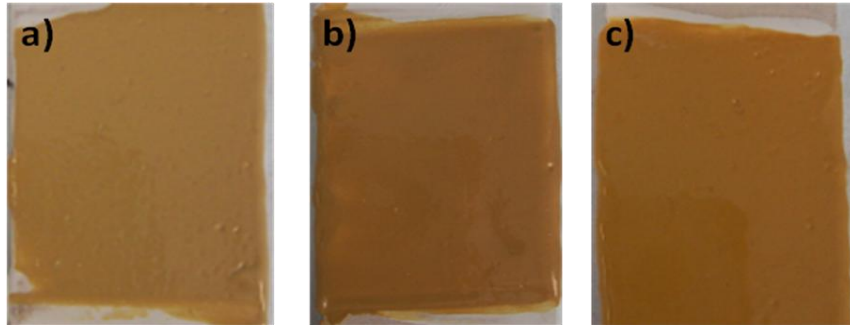


Fig. 9.

Table 1. Different treatment conditions to obtain rutile (R) or anatase (A) phase

Ref.	Urea(g)/Pigment(g)	Time (h)
R1	1.5	17
R2	1.5	24
R3	1.5	48
A1	4.5	17
A2	4.5	24
A3	4.5	48

Table 2. Frit composition

Composition (wt%) ^a						
SiO ₂	Al ₂ O ₃	RO ^b	R ₂ O ^b	ZnO	ZrO ₂	Temperature /°C
67	13	9.4	10	0.4	0.2	1080

^a The percentages do not represent quantitative analyses

^b R = alkaline or alkaline earth metals

Table 3. Chromatic coordinates of Al powder samples at different temperatures.

	L*	a*	b*
180°C (Al)	93	-5	21
750°C	78	0	23
800°C	76	1	23
850°C	77	3	28
900°C	77	5	31
1000°C	72	8	31
1080°C	70	14	36

Table 4. CIELab parameters of R2 and A1 samples after glazing (frit). CIELab parameters of a commercial ceramic pigment are included as comparison.

Powder/Glaze 1080°C			
	L*	a*	b*
R2	65	12	39
A1	64	16	41
Commercial (>1200°C)	60	16	47